S. T. Hussain, Rizwan Ul Haq*, N. F. M. Noor and S. Nadeem

Non-linear Radiation Effects in Mixed Convection Stagnation Point Flow along a Vertically Stretching Surface

DOI 10.1515/ijcre-2015-0177

Abstract: Present phenomenon is dedicated to analyze the combine effects of linear and non-linear Rosseland thermal radiations for stagnation point flow along a vertically stretching surface. For better variation in fluid flow and heat transfer, mixed convection is also considered to sustain this mechanism for significant influence. After incorporating these effects, the pertinent mathematical model is constructed in the form of non-linear partial differential equations and then be transformed into the system of coupled ordinary differential equations with the help of similarity transformation to be further solved numerically. Significant difference in the heat transfer enhancement can be observed through temperature profiles and tables of Nusselt number. Though histogram and isotherms plots, finally it is concluded that non-linear radiation provides better heat transfer rate at the surface of sheet as compare to the linear or absence of radiation effects.

Keywords: non-linear radiation, mixed convection, heat transfer, buoyancy effect, numerical solution

1 Introduction

The radiations can be visible, infrared or sun light and their visibility depends upon the nature of the material emitting from these radiations. The source of energy and its technology is mostly categorized as either passive solar or active solar depending on the way to seize and distribute of solar energy or convert it into solar power. Electromagnetic emissions from a surface with temperature greater than absolute zero are known as thermal radiations. These radiations can be visible, infrared or sun light and their visibility depends upon the nature of the material emitting these radiations. Since last few decay once of the major concern in field of science and technology a prominent source of renewable energy and its technologies are mostly categorized as either passive solar or active solar depending on the way to seize and distribute of solar energy or convert it into solar power. Viskant and Grosh (1962) noted that these radiations become important factor when considering the cooling systems, hypersonic flights, combustion chambers and power plants. They discussed the thermal radiation effects for the Falkner-Skan flow by using the Rosseland approximations (Rosseland 1931). Smith (1952) was one of the earliest scientists who discussed the radiation effects for a boundary layer flow. Perdikis and Raptis (1996) discussed the heat transfer phenomenon for micropolar fluid past a flat surface by considering the linearized form of Rosseland approximation. Later on several authors citing their work used the linearized form of Rosseland approximation to discuss the boundary layer flows in the presence of thermal radiation. Recently Bataller (2008) discussed the Blasius flow in the presence of radiation effects and found that thermal radiation effect expands the temperature distribution, but this effect starts decreasing for large values of radiation parameter. Hussain et al. (2013) examined the radiation effects on the unsteady boundary layer flow of a micropolar fluid over a stretching surface. They concluded that the micropolar fluid temperature increases with an increase in the radiation parameter. Pal and Mondal (2012) investigated the radiation and chemical reaction effects on the stretching sheet flow in a Darcian porous medium. They also observed the effect of porous medium where the temperature increases with an increase in the radiation parameter. Chen (2010) produced the analytical solution for viscoelastic fluids (Walters B fluid and second grade fluid) by considering the thermal radiations. He used the linearized form of Rosseland approximation to examine the radiation effects. They found that Nusselt number decreases with an increase in the radiation parameter.

***Corresponding author: Rizwan Ul Haq,** Department of Mathematics, Capital University of Science and Technology, Islamabad 44000, Pakistan, E-mail: ideal_riz@hotmail.com
S. T. Hussain, DBS&H, College of electrical and mechanical engineering, National University of Science & Technology, Islamabad 44000, Pakistan.
N. F. M. Noor, Institute of Mathematical Sciences, Faculty of Science, University of Malaya, 50603 Kuala Lumpur, Malaysia
S. Nadeem, Department of Mathematics, Quaid-I-Azam University, Islamabad 44000, Pakistan

A radiation effect for the fluid flow over unsteady stretching sheet has been discussed by Aziz (2009). He concluded that radiation effects are more prominent for small values of Prandtl number while Nusselt number variation is prominent for large Prandtl number. He also discussed that radiation effects are more pronouncing for steady fluid flow as compared to unsteady fluid flow. Das, Duari, and Kundu (2014) extended the work of Aziz (2009) for the nano fluid flow by considering the Buongiorno fluid model (Buongiorno 2006). They reported that radiation parameter has similar effects in the case of nanofluid flow. Several other articles (Hayat et al. 2012, 2014; Ishak, Nazar, and Pop 2006; Mahapatra and Gupta 2001, 2002; Nazar et al. 2004; Shehzad, Alsaedi, and Hayat 2013; Shehzad, Hayat, and Alsaedi 2015; Shehzad et al. 2014) can also be referred on the use of linear Rosseland approximation to discuss the radiation effects. The linear Rosseland approximation results are valid only for small temperature differences between the plate and ambient fluid. Recently Magyari (Magyari 2010; Magyari and Pantokratoras 2011) proved that for the linear Rosseland approximation case, the problem can be governed by a single effective Prandtl number instead of different parameters. So Fang and Pantokratoras (2014) recently published a short note on the Blasius flow with the non-linear radiations. The governing equation contains three parameters Prandtl number, radiation parameter and temperature parameters instead of the single parameter (effective Prandtl number). They also stated that non-linear Rosseland approximation results are valid for small as well as large temperature difference between plate and ambient fluid. The temperature profile is S-shaped for non-linear approximation when compared to linear Rosseland approximation.

After the publication of Fang and Pantokratoras article (Pantokratoras and Fang 2014), it is important to revisit the radiation effects on the fluid flows discussed earlier by using the linearized form of Rosseland approximation. The stretching sheet flows have been largely discussed by considering the radiation effects. These flows have important applications in the polymer extrusion, electric wire drawings and plastic sheets drawings. Sakiadis (1961) started the study of boundary layer flows over a continuous moving surface. Tsou, Sparrow, and Goldstein (1967) extended his work for heat transfer and Erickson, Fan, and Fox (1966) extended it for the mass transfer with suction and injection. A rich literature (Akbar et al. 2013; Cortell 2008; Mao et al. 2015; Nandeppanavar, Vajravelu, and Abel 2011; Qing et al. 2015; Rashidi et al. 2014; Van Deynse et al. 2015; Wang et al. 2015; Yu et al. 2013) is available on the stretching sheet flows. Recently Mukhopadhyay (2013) examined the slip and radiation effects on the boundary layer flow over an exponentially stretching sheet. She used the linearized form of thermal radiation and concluded that temperature increase with radiation parameter is due to the enhanced thermal conductivity. Yazdi, Moradi, and Dinarvand (2013) considered three nanoparticles to examine the effect of radiation parameter on the nanofluid flow over stretching sheet. They showed that for copper particles, the temperature increases with the increase in radiation parameter. Their graph shows temperature is increasing with the increase in magnetic and radiation parameters. The above mentioned studies used the linearized form of Rosseland approximation to examine the radiation effects.

The main motivation of present study is to highlight the concept of non-linear Rosseland approximation for mixed convection stagnation point flow along a vertically moving surface. Presently no extensive literature has been discussed for non-linear radiation. So the main purpose of the present study is to modify the concept of linear radiation to non-linear radiation effects on the stagnation point flow. Thus the mathematical model is constructed based on above mentioned analysis in Section 2. Methodology to solve the problem is defined in Section 3. In Section 4, comparison results are presented to verify our study with the existing literature and the graphs are plotted to discuss the effects of physical parameters. Additionally, histograms of local Nusselt number and the flow isotherms on the effects of non-linear radiation as compared to linear radiation and absence of radiation are included. Lastly, key findings of the whole analysis are described in Section 5.

2 Mathematical formulation

We consider the steady two dimensional fluid flow and heat transfer over a continuously moving surface. The surface is moved with the linear velocity $U_w = cx$. Moreover, we are considering the stagnation point flow with $U_\infty = bx$. The surface movement will cause the boundary layer formation. Considering the Cartesian coordinate system, fluid flow velocity will vary along x and y axis. Boundary layer equations governing the fluid flow are given by

$$\frac{\partial u}{\partial x} + \frac{\partial v}{\partial y} = 0, \tag{1}$$

$$u\frac{\partial u}{\partial x} + v\frac{\partial u}{\partial y} = U_\infty \frac{dU_\infty}{dx} + \nu\frac{\partial^2 u}{\partial y^2} \pm g\beta(T - T_\infty), \tag{2}$$

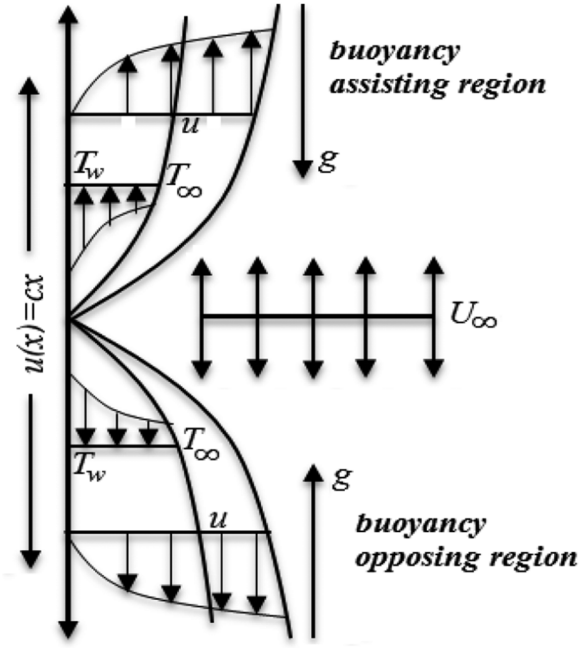

Figure 1: Geometry of the problem.

$$u\frac{\partial T}{\partial x}+v\frac{\partial T}{\partial y}=\alpha\frac{\partial^2 T}{\partial y^2}-\frac{1}{\rho c_p}\frac{\partial q_r}{\partial y}. \tag{3}$$

In above equations, $u(x,y)$ and $v(x,y)$ are the velocity components in the fluid flow and they are in perpendicular direction respectively. Here $\nu=\mu/\rho$ is kinematic viscosity, ρ is density, μ is dynamic viscosity, g is acceleration due to gravity, β is coefficient of thermal expansion, $\alpha=k/\rho c_p$ is thermal diffusivity, k is thermal conductivity, c_p is specific heat at constant pressure and q_r is radiation heat flux. The corresponding boundary conditions are given by

$$u=U_w=cx, v=0, T=T_w \text{ at } y=0, \tag{4}$$

$$u=U_\infty=ax, T=T_\infty \text{ at } y\to\infty. \tag{5}$$

The radiation heat flux can be defined by using the Rosseland approximation (Rosseland 1931)

$$q_r=-\frac{4}{3a_r}\nabla e_b, \tag{6}$$

where e_b is the rate of radiation emitted by each square meter of surface and a_r is the Rosseland mean absorption coefficient. The term $e_b=\sigma_{SB}T^4$ is defined by using Stefan-Boltzmann radiation law. This law states that all objects with temperature above absolute zero emit radiations at the rate proportional to the fourth power of its absolute temperature. So σ_{SB} is the well-known Stefan-Boltzmann constant. After using these relations, Eq. (3) can be rewritten as

$$u\frac{\partial T}{\partial x}+v\frac{\partial T}{\partial y}=\frac{\partial}{\partial y}\left\{\left(\alpha+\frac{16\sigma_{SB}T^3}{3\rho c_p a_r}\right)\right\}\frac{\partial T}{\partial y}. \tag{7}$$

The above equation is highly non-linear in T. The major simplification can be done if the temperature difference between wall and fluid is small. In that case, T can be replaced by T_∞ but the obtained results will be valid only when temperature gradient within the flow is small. Introducing the following transformations in the governing equations and boundary conditions

$$u=\frac{\partial\psi}{\partial y}, v=-\frac{\partial\psi}{\partial x}, \eta=y\sqrt{\frac{c}{\nu_f}}, f(\eta)=\frac{\psi}{x\sqrt{c\nu_f}}, \theta(\eta)=\frac{T-T_\infty}{T_w-T_\infty}. \tag{8}$$

Hence we get

$$f'''+ff''-f'^2+r^2\pm\lambda\theta=0, \tag{9}$$

$$\theta''+Prf\theta'+\frac{N_r}{3(1-\theta_r)}\left[((1-\theta_r)\theta+\theta_r)^4\right]''=0, \tag{10}$$

$$f(0)=0, f'(0)=1, f'(\infty)=r=a/c, \tag{11}$$

$$\theta(0)=1, \theta(\infty)=0, \tag{12}$$

where

$$Nr=4\sigma_{SB}{T_w}^3/ka_r, \theta\hat{r}=T_\infty/T_w, \lambda=Gr_x/\mathrm{Re}_x \tag{13}$$

The value of θ_r is the ratio of ambient fluid temperature to temperature at wall and it is noticeable that it can be greater than or less than one. In such cases when θ_r is equal to one, there is no temperature difference between the wall and the ambient fluid. The constant $\lambda(\geq 0)$ in the equation (9) is the buoyancy parameter with $Gr_x=g\beta(T_w-T_\infty)x^3/\nu^2$ is the local Grashof number and $\mathrm{Re}_x=U_wx/\nu$ is the local Reynolds number, so the system will be in thermal equilibrium. The definition of θ_r is somewhat different from (Hayat et al. 2012) due to difference in the temperature transformations. Physical quantities of interest are the skin friction coefficient and the local Nusselt number

$$c_f=\frac{\tau_w}{\rho U_w^2/2}, Nu=\frac{x(q_w+q_r)}{k(T_w-T_\infty)}, \tag{14}$$

where $\tau_w=\left[\mu\frac{\partial u}{\partial y}\right]_{y=0}$ and $q_w=-k\left(\frac{\partial T}{\partial y}\right)_{y=0}$. Using transformation (8) and $Re=\frac{U_wx}{\nu}$, we have

$$\frac{1}{2}C_fRe_x^{1/2}=f''(0), \tag{15}$$

$$Re_x^{-1/2}Nu=-\left[\frac{4}{3}(N_r(1-\theta_r)\theta(0)+\theta_r)^3+1\right]\theta'(0) \tag{16}$$

3 Methodology

Equations (9) and (10) combined with the boundary conditions (11) and (12) are solved numerically using a Runge-Kutta (RK) method of order fourth-fifth along with the shooting technique. The step size is taken as $\Delta\eta = 0.01$ and the convergence criteria is set at 10^{-6}. The asymptotic boundary conditions given by Eq. (12) were replaced by using a value of similarity variable $\eta_{\max} = 12$ as follows:

$$f'(\eta_{\max}) = \text{and } \theta(\eta_{\max}) = 0. \tag{17}$$

The choice of $\eta_{\max} = 12$ ensures that all numerical solutions approached the asymptotic values correctly. Further detail of the methodology is described in the books by Na (1979) and Cebeci and Bradshaw (1984).

4 Results and discussion

In this section, comparisons between present results with solutions by different authors are listed in Tables 1 and 2. Good agreements are achieved in these findings. The variations of the flow local Nusselt number in the absence of radiation, with linear radiation and with non-linear radiation are also tabulated in Table 3. It is found that the local Nusselt number is escalated by multiplying the values of the buoyancy parameter λ for assisting flow, the thermal radiation parameter Nr and the ratio of the fluid temperature θ_r. Besides we will discuss the effects of the aforementioned significant parameters including the stagnation parameter r towards the velocity and temperature profiles of assisting and opposing components of the mixed convective stagnation point flow. The variations of local skin friction and local Nusselt number towards the buoyancy parameter λ along with the influence of some other contributing parameters are also demonstrated graphically for both driven flows.

In the context of stagnation flow model, buoyancy parameter represents a dispersive force which is caused by the pressure difference between the tip of a flow body and depth or length of the flow column as it collides with a static surface. Generally when the buoyancy parameter, in this case, λ increases, the rate of amount of displaced fluid will be greater which may provokes the velocity of the flow to be higher as depicted in Figure 2(a). Furthermore it is shown in Figure 2(b) that the flow

Table 1: Comparison for skin friction coefficient and local Nusselt number when $Nr = M = \theta_r = \lambda = 0$.

$r \downarrow$	$C_f Re_x^{1/2}$				$Nu_x Re_x^{-1/2}$ (When $Pr = 1.5$)	
	Mahapatra and Gupta (2001, 2002)	Nazar, Amin, Filip and Pop, (2004)	Ishak, Nazar, and Pop (2006)	Present	Mahapatra and Gupta (2001, 2002)	Present
0.1	−0.9694	−0.9694	−0.9694	−0.9694	−0.777	−0.7768
0.2	−0.9181	−0.9181	−0.9181	−0.9181	−0.797	−0.7971
0.5	−0.6673	−0.6673	−0.6673	−0.6673	−0.863	−0.8648
2.0	2.0175	2.0176	2.0175	2.0175	−1.171	−1.1781
3.0	4.7293	4.7296	4.7294	4.7293	−1.341	−1.3519

Table 2: Comparison for skin friction coefficient and local Nusselt number when $Nr = M = \theta_r = 0$ and $\lambda = r = 1$.

$Pr \downarrow$	Assisting flow				Opposing flow			
	$C_f Re_x^{1/2}$		$Nu_x Re_x^{-1/2}$		$C_f Re_x^{1/2}$		$Nu_x Re_x^{-1/2}$	
	Ishak, Nazar, and Pop (2006)	Present	Ishak, Nazar, and Pop (2006)	Present	Ishak, Nazar, and Pop (2006)	Present	Ishak, Nazar, and Pop (2006)	Present
0.72	0.3645	0.3644	1.0931	1.0931	−0.3852	−0.3853	1.0293	1.0293
6.8	0.1804	0.1804	3.2902	3.2902	−0.1832	−0.1832	3.2466	3.2467
20	0.1175	0.1175	5.6230	5.6230	−0.1183	−0.1183	5.5923	5.5924
40	0.0873	0.0875	7.9463	7.9463	−0.0876	−0.0877	7.9227	7.9229
60	0.0729	0.0731	9.7327	9.7327	−0.0731	−0.0731	9.7126	9.7125
80	0.0640	0.0641	11.2413	11.2413	−0.0642	−0.0640	11.2235	11.2236

Table 3: Variation of local Nusselt number when $r = 0.5$ and $Pr = 6.2$.

$\theta_r \downarrow$	$Nr \downarrow$	Effects ↓	$Nu_x Re_x^{-1/2}$					
			Assisting flow			Opposing flow		
			$\lambda = 0$	$\lambda = 0.5$	$\lambda = 1$	$\lambda = 0$	$\lambda = 0.5$	$\lambda = 1$
0	0	Absence of radiation	1.858078	1.872872	1.887049	1.858078	1.842592	1.826322
0	1	Linear radiation	2.254163	2.279113	2.302693	2.254163	2.227618	2.199187
0	5		3.309659	3.383624	3.45032	3.309659	3.226013	3.128616
0	10		4.198182	4.341054	4.464385	4.198182	4.025396	3.798588
0.25	10	Non-linear radiation	4.558999	4.734964	4.884342	4.558999	4.339902	4.032483
0.5	10		5.029013	5.248957	5.432395	5.029013	4.745911	4.309840
1.5	10		11.15610	11.30510	11.44646	11.1561	10.99834	10.83040

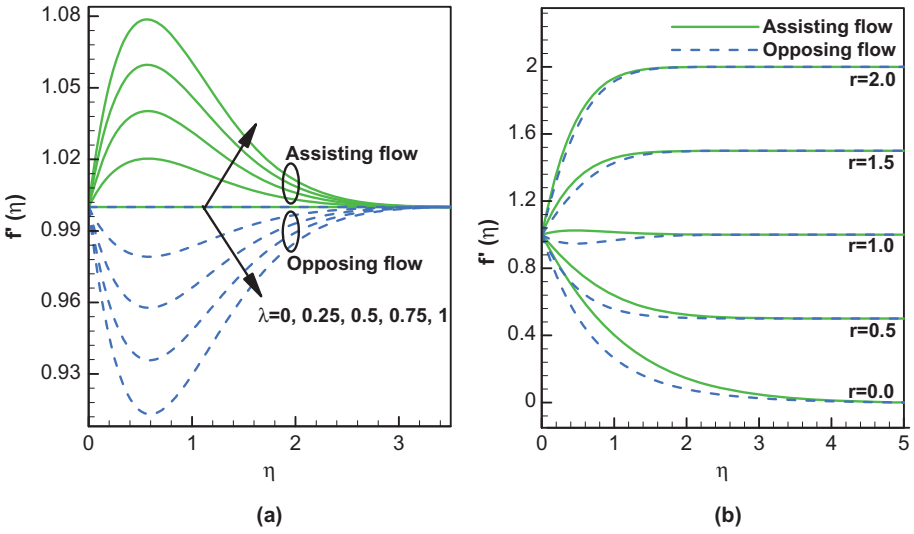

Figure 2: Velocity profiles when $\theta_r = 1.5$, $Pr = 6.2$, $Nr = 0.5$ while (a) $\lambda(r = 1)$ and (b) r $(\lambda = 0.5)$ are varied.

speed can be amplified with a slight rise in the stagnation parameter r which possibly attributed by enhanced stagnation pressure on the boundary surface. On the other hand, increasing the buoyancy parameter λ and the stagnation parameter r leads to reduction in the flow temperature as evidenced in Figure 3. This phenomenon is concurrently caused by augmentation in velocity which suggests more heat can be transferred from the flow to surroundings thus cooling down the flow.

The effects of thermal radiation parameter Nr and the ratio of ambient temperature towards wall temperature θ_r in the flow velocity and temperature distributions are captured in Figures 4 and 5 respectively. Since Nr represents thermal dissipation via electromagnetic emissions, the flow main energy is converted to electromagnetic energy that fosters the internal kinetic movements and collisions between the fluid molecules. Therefore with advancement in the thermal radiation value Nr, the flow slows down in Figure 4(a) but the internal conductivity of the fluid directs the fluid flow to be hotter as displayed in Figure 5(a). Apparently as the value of θ_r becomes greater, the temperature gradient also amplifies provided other variables in the system remain unaltered. Thus the flow temperature declines rapidly with an increase in θ_r as configured in Figure 5(b). Falling off temperature suggests loosing of energy in the boundary layer flow. As a result, the flow velocity decays accordingly with θ_r in Figure 4(b). It is learnt here that except for the stagnation parameter r, the buoyancy parameter λ, the thermal radiation N_r and the temperature ratio θ_r exhibit symmetrical effects to the velocity profiles occupying both directions of assisting and opposing flows.

Further impacts of the stagnation parameter r and the buoyancy parameter λ are analyzed in the graphical scatterings of the flow local skin friction and local Nusselt number in Figure 6. Based on Newton's law, an

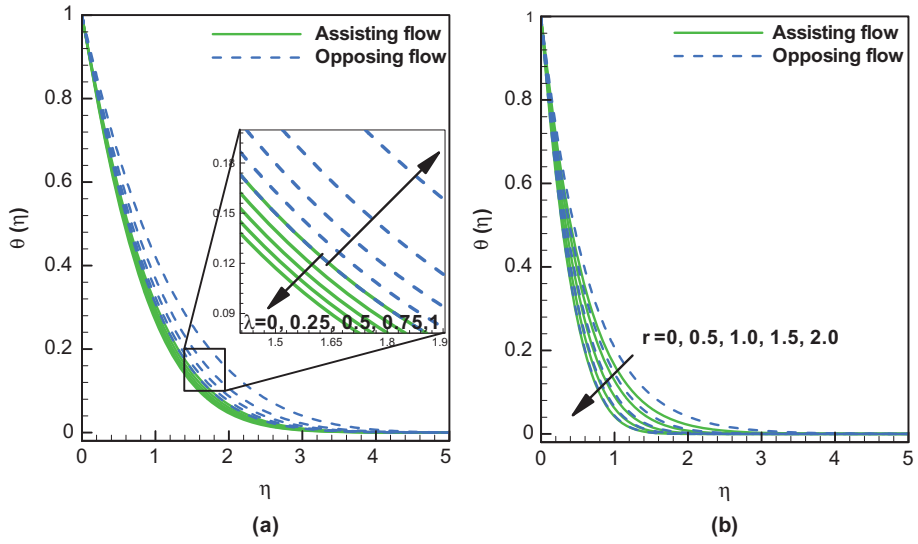

Figure 3: Temperature profiles when $\theta_r = 1.5$, $Pr = 6.2$, $Nr = 0.5$ while (a)λ ($r = 0.5$) and (b) r ($\lambda = 0.5$) are varied.

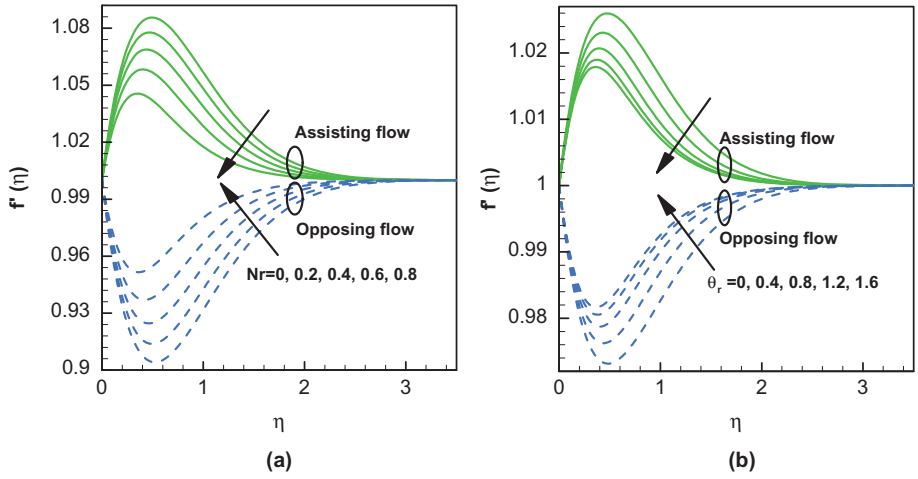

Figure 4: Velocity profiles when $r = 1$, $Pr = 6.2$, $\lambda = 0.5$ while (a) $Nr(\theta_r = 1.5)$ and (b) θ_r ($Nr = 0.5$) are varied.

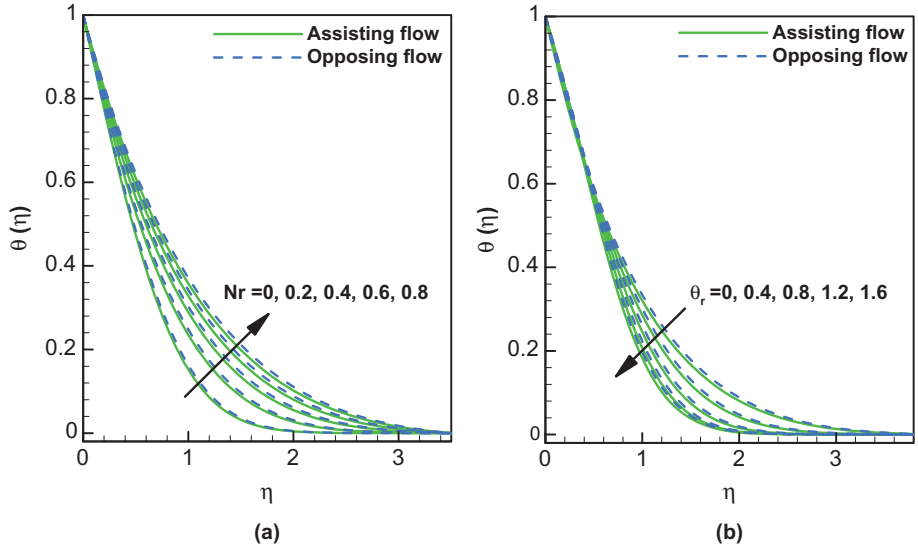

Figure 5: Temperature profiles when $r = 1$, $Pr = 6.2$, $\lambda = 0.5$ while (a) Nr ($\theta_r = 1.5$) and (b) θ_r ($Nr = 0.5$) are varied.

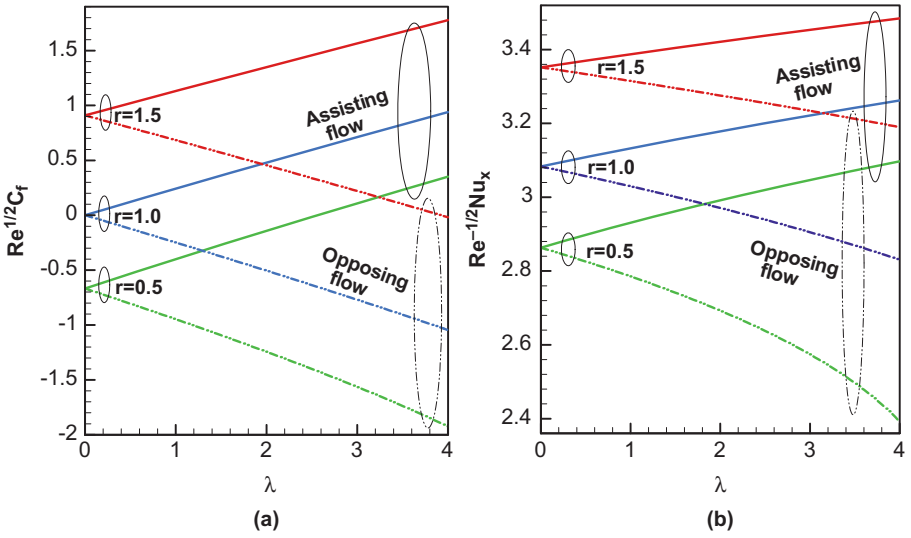

Figure 6: Profiles of (a) local skin friction and (b) local Nusselt number when and r is varied.

addition of force in one direction impinges on addition of force in other direction to synchronize the existing forces. Since the flow travels faster under greater control of r and λ as verified in Figure 2, then the skin friction countering the flow direction also increases as shown in Figure 6(a). Hence, the local Nusselt number (Figure 6(b)) which denotes the rate of heat transferred to surroundings ascends in consequence with the waning flow temperature in Figure 3(b).

Next the bearings of the buoyancy parameter λ along the Prandtl number Pr and the radiation parameter Nr towards the local Nusselt number are presented in Figure 7. The values of $Pr = 3.97$, $Pr = 6.2$ and $Pr = 14.2$ are specifically chosen to typify three base fluids i.e. acetone, water and ethanol respectively. It is found that by elevating the Prandtl number, the local Nusselt number is sloping up. Physical justification behind this occurrence may lies in the definition of Prandtl number being the ratio of viscous diffusivity against thermal conductivity. Rising of Pr indicates reduction in thermal conductivity which implies the internal ability of the flow to hold the energy is weakening as inversely proportional to the heat flux as observed in Figure 7(a). Apparently, the impulse of the radiation parameter Nr towards the local Nusselt number is quite eccentric. Based on Figures 4(a) and 5(a), it is understood that the flow experiences

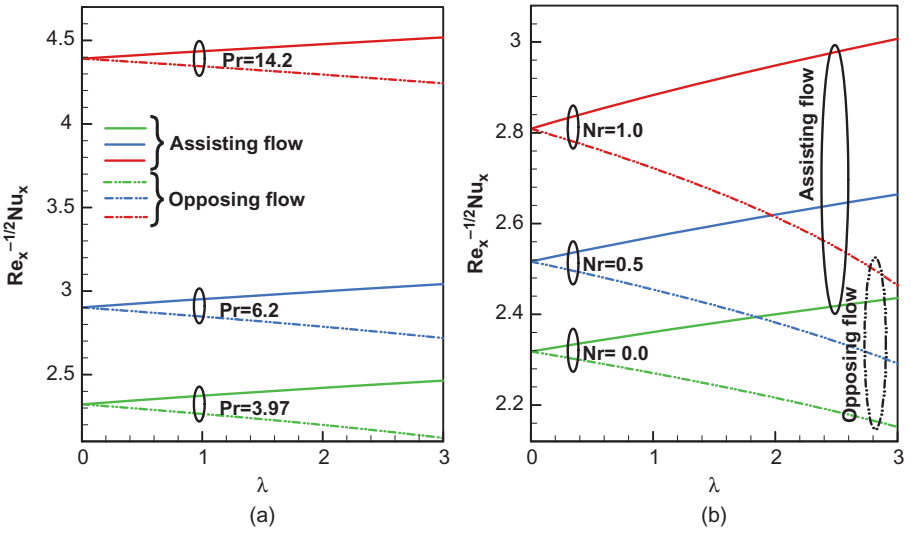

Figure 7: Profiles of local Nusselt number when $r = 0.5$, $\theta_r = 1.5$ while (a) $Pr(Nr = 0.5)$ and (b) Nr $(Pr = 6.2)$ are varied.

vanishing momentum in the movement but growing temperature at the same time due to supplement of internal kinetic collisions between fluid molecules when *Nr* inclines. Yet this incidence does not obstruct the spreading rate of heat transport from the flow to the vicinity as revealed in Figure 7(b).

Eminent impact of non-linear thermal radiation towards the local Nusselt number as compared to the effects of linear radiation and absence of radiation can better be perceived from the following histograms in Figure 8 (assisting flows) and Figure 9 (opposing flows) respectively. Through these figures, it can be observed that in the absence of radiation effect there is no variation in the local Nusselt number however by incorporating the linear radiation effect, the local Nusselt number is gradually increasing with an increase in the value of the linear radiation parameter *Nr*. Moreover, the variation in the local Nusselt number is rapidly increasing by incorporating the combined effects of both linear and non-linear radiation parameters. To analyze the fluid flow behavior, stream lines are plotted in Figure 10 within the restricted domain. These stream lines are plotted for two different cases (a) in the absence of stagnation point and (b) in the presence of stagnation point. Since stagnation parameterris ratio of stagnation point "*a*" to the stretching sheet "*c*" so in the absence of stagnation provides more dominant effects of stretching at the fluid. However, fluid is about to stagnant at the free stream when the effects of stagnation point are more dominant as compare to stretching sheet. After analyzing the behavior of fluid flow, isotherms are plotted in Figure 11 for three different cases (absence of radiation, linear radiation and non-

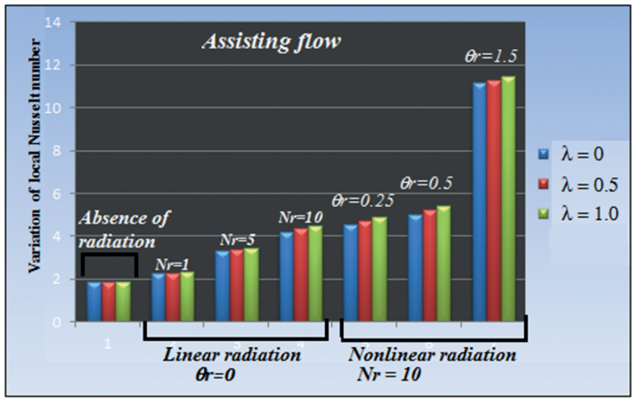

Figure 8: Variation of local Nusselt number due to non-linear radiation effects as compared to linear radiation and absence of radiation for assisting flows.

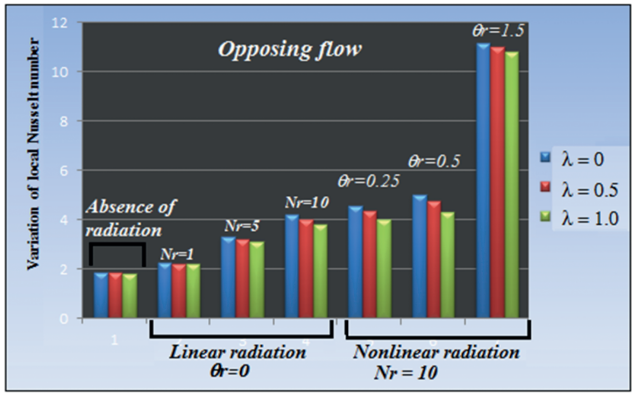

Figure 9: Variation of local Nusselt number due to non-linear radiation effects as compared to linear radiation and absence of radiation for opposing flows.

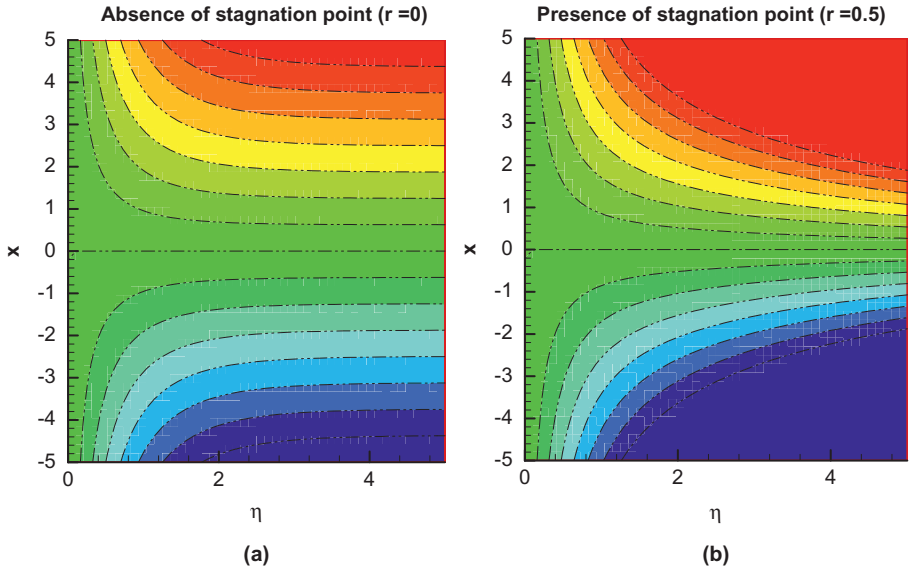

Figure 10: Variation of stream lines when (a) $r = 0$ (b) $r = 0.5$.

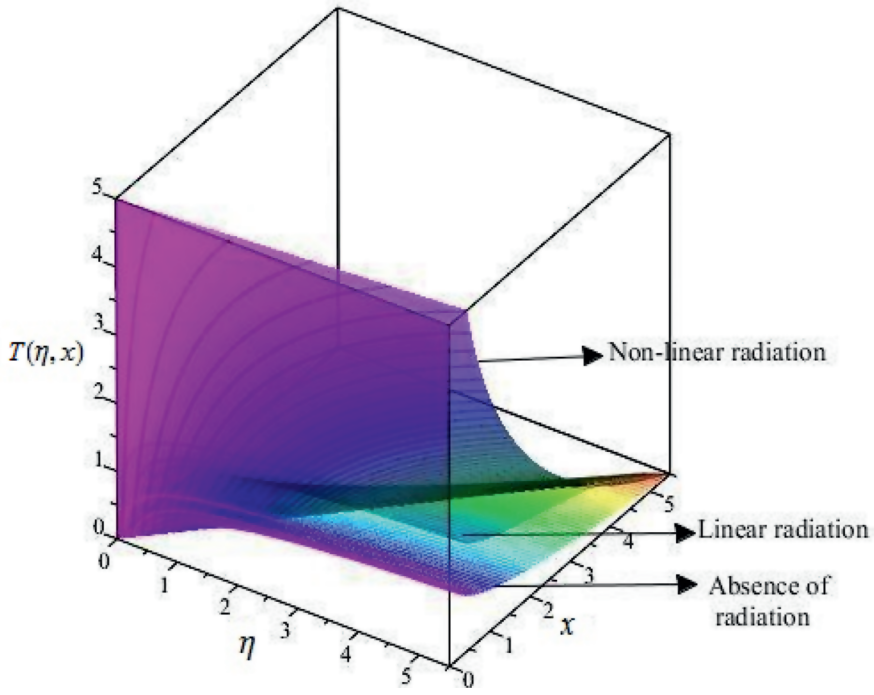

Figure 11: The flow isotherms due to non-linear radiation effects as compared to linear radiation and absence of radiation.

linear radiation). It is finally concluded that significant difference in the variation of thermal contour lines is based on radiation effect and high heat transfer has been achieved in the case of non-linear thermal radiation.

5 Conclusion

The mixed convection of a thermal radiative stagnation point flow on a vertically stretching sheet is investigated in this study. This problem is solved numerically using the shooting technique with Runge-Kutta method of fourth-fifth order. The following conclusions are drawn:

- Both the buoyancy and stagnation parameters tend to increase the velocity distributions and to decrease the temperature distributions simultaneously.
- The effects of thermal radiation parameter to the model is fully opposite with the buoyancy and stagnation parameters due to growing internal kinetics movement of fluid molecules as the flow thermal energy is converted to electromagnetic emissions.
- Symmetrical patterns for assisting and opposing flows in the velocity profiles can be spotted for all examined parameters excluding the stagnation parameter r.
- Higher ratio of ambient temperature towards wall temperature caused both the velocity and temperature profiles to decline.
- The local skin frictions of this stagnation flow are raised by escalating the buoyancy and stagnation parameters.
- The buoyancy parameter affects the temperature profile with adverse directions of assisting and opposing flows while causing the local Nusselt number to incline under influence of rising values of the stagnation and thermal radiation parameters, the ratio of fluid temperature θ_r and also the Prandtl number.
- The variation of local Nusselt number is highly affected by the combined effects of both linear and non-linear thermal radiations based on the histograms.
- The isotherms of the flow are significantly dominated by the non-linear thermal radiation effect.

References

1. Akbar, N.S., Nadeem, S., Ul Haq, R., Khan, Z.H., 2013. Radiation Effects on MHD Stagnation Point Flow of Nano Fluid Towards a Stretching Surface with Convective Boundary condition. Chinese J. Aeronaut. 26, 1389–1397.
2. Bataller, R.C., 2008. Radiation Effects in the Blasius Flow. Appl. Math. Comput. 198, 333–338.
3. Buongiorno, J., 2006. Convective Transport in Nanofluids. J. Heat Transf. 128, 240–250.
4. Cebeci, T., Bradshaw, P., 1984. Physical and Computational Aspects of Convective Heat Transfer, Springer-Verlag, New York.

5. Chen, C.H., 2010. On the Analytic Solution of MHD Flow and Heat Transfer for Two Types of Viscoelastic Fluid Over a Stretching Sheet with Energy Dissipation, Internal Heat Source and Thermal Radiation. Int. J. Heat Mass Transf. 53, 4264–4273.
6. Cortell, R., 2008. Effects of Viscous Dissipation and Radiation on the Thermal Boundary Layer Over a Nonlinearly Stretching Sheet. Phys. Lett. A 372, 631–636.
7. Das, K., Duari, P.R., Kundu, P.K., 2014. Nanofluid Flow Over an Unsteady Stretching Surface in Presence of Thermal Radiation. Alexandria Eng J. http://dx.doi.org/10.1016/j.aej.2014.05.002.
8. El-Aziz, M.A., 2009. Radiation Effect on the Flow and Heat Transfer Over an Unsteady Stretching Sheet. Int. Commun. Heat Mass Transf. 36, 521–524.
9. Erickson, L.E., Fan, L.T., Fox, V.G., 1966. Heat and Mass Transfer in the Laminar Boundary Layer Flow of a Moving Flat Surface with Constant Surface Velocity and Temperature Focusing on the Effects of Suction/Injection. Ind. Eng. Chem. 5, 19–25.
10. Hayat, T., Shehzad, S.A., Qasim, M., Obaidat, S., 2012. Radiative Flow of Jeffery Fluid in a Porous Medium with Power Law Heat Flux and Heat Source. Nucl. Eng. Des. 243, 15–19.
11. Hussain, M., Ashraf, M., Nadeem, S., Khan, M., 2013. Radiation Effects on the Thermal Boundary Layer Flow of a Micropolar Fluid Towards a Permeable Stretching Sheet. J. Franklin Inst. 350, 194–210.
12. Hussain, T., Shehzad, S.A., Hayat, T., Alsaedi, A., Al-Solamy, F., et al., 2014. Radiative Hydromagnetic Flow of Jeffrey Nanofluid by an Exponentially Stretching Sheet. PLoS ONE 9, e103719. doi: 10.1371/journal.pone.0103719.
13. Ishak, A., Nazar, R., Pop, I., 2006. Mixed Convection Boundary Layers in the Stagnation-Point Flow Towards a Stretching Vertical Sheet. Meccanica 41, 509–518.
14. Magyari, E., 2010. Comment on Mixed Convection Boundary Layer Flow Over a Horizontal Plate with Thermal Radiation. Heat Mass Transf. 46, 809–810. doi:10.1007/s00231-010-0639-x.
15. Magyari, E., Pantokratoras, A., 2011. Note on the Effect of Thermal Radiation in the Linearized Rosseland Approximation on the Heat Transfer Characteristics of Various Boundary Layerflows. Int. Commun. Heat Mass Transf. 38, 554–556.
16. Mahapatra, T.R., Gupta, A.S., 2001. Magnetohydrodynamic Stagnation-Point Flow Towards a Stretching Sheet. Acta Mech. 152, 191–196.
17. Mahapatra, T.R., Gupta, A.S., 2002. Heat Transfer in Stagnation-Point Flow Towards a Stretching Sheet. Heat Mass Transf. 38, 517–521.
18. Mao, Y., Li, Z., Feng, K., Guo, X., Zhou, Z., Dong, J., Wu, Y., 2015. Preparation, Characterization and Wear Behavior of Carbon Coated Magnesium Alloy with Electroless Plating Nickel Interlayer. Appl. Surf. Sci. 327, 100–106.
19. Mukhopadhyay, S., 2013. Slip Effects on MHD Boundary Layer Flow Over an Exponentially Stretching Sheet with Suction/ Blowing and Thermal Radiation. Ain. Shams. Eng. J. 4, 485–491.
20. Na, T.Y., 1979. Computational Methods in Engineering Boundary Value Problem, Academic Press, New York.
21. Nandeppanavar, M.M., Vajravelu, K., Abel, M.S., 2011. Heat Transfer in MHD Viscoelastic Boundary Layer Flow Over a Stretching Sheet with Thermal Radiation and Non-Uniform Heat Source/Sink. Commun. Nonlinear Sci. Numer. Simulat. 16, 3578–3590.
22. Nazar, R., Amin, N., Filip, D., Pop, I., 2004. Unsteady Boundary Layer Flow in the Region of the Stagnation Point on a Stretching Sheet. Int. J. Eng. Sci. 42, 1241–1253.
23. Pal, D., Mondal, H., 2012. Influence of Chemical Reaction and Thermal Radiation on Mixed Convection Heat and Mass Transfer over a Stretching Sheet in Darcian Porous Medium with Soret and Dufour Effects. Energ. Convers. Manage. 62, 102–108.
24. Pantokratoras, A., Fang, T., 2014. Blasius Flow with Non-Linear Rosseland Thermal Radiation. Meccanica. June 2014, 49, 1539–1545. doi: 10.1007/s11012-014-9911-3.
25. Perdikis, C., Raptis, A., 1996. Heat Transfer of a Micropolar Fluid by the Presence of Radiation. Heat Mass Tranf. 31, 381–382.
26. Qing, Z., Haixia, L., Huali, Li., Yu, L., Huayong, Z., Tianduo, Li., 2015. Solvothermal Synthesis and Photocatalytic Properties of NiO Ultrathin Nanosheets with Porous Structure. Appl. Surf. Sci.328, 525–530.
27. Rashidi, M.M., Rostami, B., Freioonimehr, N., Abbasbandy, S., 2014. Free Convective Heat and Mass Transfer for MHD Fluid Flow Over a Permeable Vertical Stretching Sheet in the Presence of the Radiation and Buoyancy Effects. Ain. Shams. Eng. J. 5, 901–912.
28. Rosseland, S., 1931. Astrophysikaud atom-theoretischegrundlagen, Springer, Berlin, pp. 41–44.
29. Sakiadis, B.C., 1961. Boundary Layer Behavior on Continuous Solid Flat Surfaces. Am. Inst. Chem. Eng. J. 7, 26–28.
30. Shehzad, S.A., Alsaedi, T., Hayat, T., 2013. Influence of Thermophoresis and Joule Heating on the Radiative Flow of Jeffrey Fluid with Mixed Convection. Braz. J. Chem. Eng. 30, 897–908. doi: 10.1590/s0104-66322013000400021.
31. Shehzad, S.A., Hayat, T., Alsaedi, A., 2015. Influence of Convective Heat and Mass Conditions in MHD Flow of Nanofluid. Bull.Pol. Acad. Sci. Techn. Sci.63, 465–474.
32. Shehzad, S.A., Hayat, T., Alsaedi, A., Obid, M.A., 2014. Nonlinear Thermal Radiation in Three-Dimensional Flow of Jeffrey Nanofluid: A Model for Solar Energy. Appl. Math. Comput. 248, 273–286.
33. Smith, W.J., 1952. Effect of Gas Radiation in the Boundary Layer on Aerodynamic Heat Transfer. J. Aero. Sci. 20, 579.
34. Tsou, F.K., Sparrow, E.M., Goldstein, R.J., 1967. Flow and Heat Transfer in the Boundary Layer on a Continuous Moving Surface. Int. J. Heat Mass Transf. 10, 219–235.
35. Van Deynse, A., Cools, P., Leys, C., De Geyter, N., Morent, R., 2015. Surface Activation of Polyethylene with an Argon Atmospheric Pressure Plasma Jet: Influence of Applied Power and Flow Rate. Appl. Surf. Sci. 328, 269–278.
36. Viskanta, R., Grosh, R.J., 1962. Boundary Layer in Thermal Radiation Absorbing and Emitting mEdia. Int. J. Heat Mass Transf. 5, 795–806.
37. Wang, R., Zhang, C., Liu, X., Xie, Q., Yan, P., Shao, T., 15 February 2015. Microsecond Pulse Driven Ar/CF_4 Plasma Jet for Polymethylmethacrylate Surface Modification at Atmospheric Pressure. Appl. Surf. Sci.328, 509–515.
38. Yazdi, M.E., Moradi, A., Dinarvand, S., 2013. Radiation Effects on MHD Stagnation-Point Flow in a Nanofluid. Res. J. Appl. Sci. Eng. Tech. 5, 5201–5208.
39. Yu, X., Huo, Y., Yang, J., Chang, S., Ma, Y., Huang, W., 2013. Reduced Graphene Oxide Supported Au Nanoparticles as an Efficient Catalyst for Aerobic Oxidation of Benzyl Alcohol. Appl. Surf. Sci.280, 450–455.